SSCL-SR-1221

SSCL-SR-1221
June 1993
Distribution Category: 414

F. Paige
A. Vanyashin

Simulation of Supersymmetry Signatures for GEM

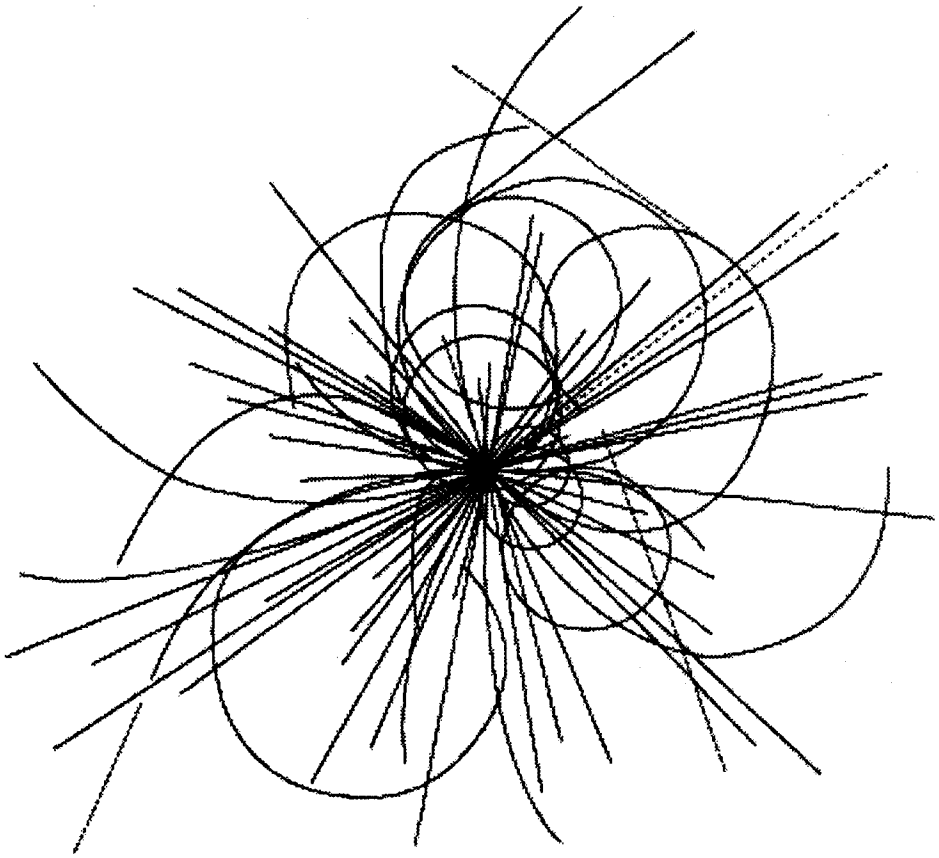

Superconducting Super Collider Laboratory

SSCL-SR-1221

Simulation of Supersymmetry Signatures for GEM

F. Paige and A. Vanyashin

Superconducting Super Collider Laboratory*
2550 Beckleymeade Ave.
Dallas, TX 75237

June 1993

*Operated by the Universities Research Association, Inc., for the U.S. Department of Energy under Contract No. DE-AC35-89ER40486.

SIMULATION OF SUPERSYMMETRY SIGNATURES FOR GEM

Frank E. Paige and A.V. Vanyashin
Physics Research Division
Superconducting Super Collider Laboratory
2550 Beckleymeade Avenue
Dallas, TX 75237

The GEM detector can observe gluinos and squarks using the signature of missing transverse energy plus multiple jets over the whole range of masses relevant to the electroweak scale. It can also observe the likesign dilepton signature for gluinos.

1. Introduction

Supersymmetry (SUSY) is theoretically attractive because it eliminates the quadratic divergences in the Higgs sector and so allows light elementary Higgs bosons to occur naturally. Its study also provides a good testing ground for many aspects of GEM,[1] including missing energy, jets and leptons. The minimal supersymmetric extension of the standard model[2] or MSSM has two Higgs doublets and superpartners (denoted by a tilde) for all normal particles. In particular there are four neutralinos, $\widetilde{\chi}_i^0$, which are linear combinations of the partners of the photon, Z, and neutral Higgs bosons, and two pairs of charginos, $\widetilde{\chi}_i^{\pm}$. If SUSY is broken at the electroweak scale, the masses of all of these particles should be less than about 1 TeV. There is a conserved R parity carried by all superparticles, so they must always be produced in pairs and decay to the lightest supersymmetric particle, which is absolutely stable. Only the minimal model with $\widetilde{\chi}_1^0$ being the lightest supersymmetric particle will be considered here. The results demonstrate that in GEM the backgrounds for these signatures are dominated by standard model physics, not by detector effects.

2. Event Simulation

The event simulation for this study is based on the minimal supersymmetric extension of the standard model[2] as implemented in ISAJET 7.00.[3] In this model there are two Higgs doublets and supersymmetric partners with $\Delta J = \pm 1/2$ for all the normal particles. The physical Higgs bosons after symmetry breaking are h, H, A, and $H^{\pm}$. Their superpartners mix with those of the γ, Z^0 and $W^{\pm}$ to give four neutralinos $\widetilde{\chi}_i^0$ and two charginos $\widetilde{\chi}_i^{\pm}$. Supersymmetric SU(5) grand unification is assumed in the chargino and neutralino mass

matrices, but the squark, left and right slepton, sneutrino, and left and right stop masses are treated as arbitrary. There is a conserved R parity, so supersymmetric particles are produced in pairs and decay to the lightest supersymmetric particle, which is assumed to be $\widetilde{\chi}_1^0$. In general the decays of gluinos and squarks involve a cascade through several $\widetilde{\chi}_i$ states.

Pairs of SUSY particles are produced using the lowest order cross sections for $\widetilde{g}\widetilde{g}$, $\widetilde{g}\widetilde{q}$, $\widetilde{q}\widetilde{q}$, $\widetilde{\chi}_i\widetilde{g}$, and $\widetilde{\chi}_i\widetilde{q}$ final states. Left and right squarks are distinguished since they have different decay modes. Approximate cross sections keeping just the W and Z contributions are also included for $\widetilde{\chi}_i^{\pm}\widetilde{\chi}_i^{\pm}$ and $\widetilde{\chi}_i^{\pm}\widetilde{\chi}_i^0$. Leading-log QCD radiation is generated in the usual way. Decay widths for all the SUSY particles are calculated according to the MSSM, the decays are generated according to phase space, and leading-log QCD radiation is added. Most calculations of decay widths are done at the tree level, but one-loop results for gluino loop decays, $H \to \gamma\gamma$, and $H \to gg$, t loop corrections to the Higgs mass spectrum and couplings, and QCD corrections to $H \to q\bar{q}$ are included. The following are not included in this version:

- Gluino decays into stops. (Stop loops are included.)
- Stop decays, which depend on additional parameters such as the soft SUSY breaking A parameter.
- Higgs decays into sleptons and squarks (which are likely small except for decays into third generation sparticles).

These will be added in a future version.

The independent parameters are taken to be the gluino mass $M_{\tilde{g}}$, the common squark mass $M_{\tilde{q}}$, the left and right stop masses $M_{\tilde{t}_L}$ and $M_{\tilde{t}_R}$, the left slepton mass $M_{\tilde{\ell}_L}$, the right slepton mass $M_{\tilde{\ell}_R}$, the sneutrino mass $M_{\tilde{\nu}}$, the ratio of vacuum values $\tan\beta = v_1/v_2$, the supersymmetric Higgs mass μ, and the pseudoscalar Higgs mass M_A. Some of these parameters are related in supergravity grand unified models.

3. $\not{E}_T$ Signature For Gluinos and Squarks

Since the lightest supersymmetric particle $\widetilde{\chi}_1^0$ is neutral and interacts weakly with matter, it escapes from the detector. Thus, one of the basic signatures for SUSY is missing transverse energy, $\not{E}_T$, from the $\widetilde{\chi}_1^0$, plus multiple jets. A stringent test for GEM's missing energy resolution is to be able to detect, in this mode, gluinos and squarks with masses as light as 300 GeV. This is near the limit expected from the Tevatron and is also the mass range expected in some SUSY grand unified models.[4,5] The MSSM typically produces cascade decays from one supersymmetric particle to another. The events can have many jets and leptons, and the missing energy from the final lightest supersymmetric particle $\widetilde{\chi}_1^0$ can be small compared to the parent mass. A typical decay sequence for a relatively light squark and gluino with $M_{\tilde{q}} > M_{\tilde{g}}$ might be

$$\begin{aligned} \widetilde{u}_L &\to \widetilde{g}u\,, \\ \widetilde{g} &\to \widetilde{\chi}_1^+\bar{u}d\,, \\ \widetilde{\chi}_1^+ &\to \widetilde{\chi}_1^0 e^+\nu\,. \end{aligned} \tag{3.1}$$

Table 1. Choices of MSSM paramaters for the three cases considered. These were chosen to have different event topologies and to span the whole mass range. All the squarks and all the sleptons are taken to be degenerate for simplicity. All masses are in GeV. See Ref. 2 for the notation.

Parameter	Case I	Case II	Case III
$M_{\tilde{g}}$	300	350	2000
$M_{\tilde{q}}$	600	325	2500
$M_{\tilde{\ell}}$	500	200	1500
M_A	300	300	300
μ	−300	−300	−1000
$\tan\beta$	2	2	2

Decay chains can be even more complex for heavier masses. All of these possible decays are included in the version of ISAJET[3] used for this analysis.

There are a number of other parameters in the MSSM besides the gluino and squark masses, and it is beyond the scope of this study to explore the MSSM parameter space completely. Instead, the representative choices listed in Table 1 have been considered. Case I has a light gluino and a heavier squark; it is generally similar to the models of Ref. 4 and to the case considered in previous GEM studies.[6] Case II has a squark slightly lighter than the gluino and is generally similar to the models of Ref. 5. Since $\tilde{g} \to \tilde{q}q$ dominates for $M_{\tilde{g}} > M_{\tilde{q}}$, the signatures in this case are similar to those for squark pair production. One might think that this case would be more difficult to detect because the events contain just two hard jets from $\tilde{q} \to \tilde{\chi}_1^0 q$. It is actually easier, because the branching ratios for $\tilde{q}_L \to \tilde{\chi}_1^{\pm} q$ and $\tilde{q}_L \to \tilde{\chi}_2^0 q$ turn out to be large and to provide multijet signatures, and the dominant decay $\tilde{q}_R \to \tilde{\chi}_1^0 q$ gives low jet multiplicity but a harder $\not{E}_T$ distribution. Finally, Case III has all the masses pushed to their highest values if SUSY is to be related to the electroweak scale. It tests the ability of GEM to cover the top of the plausible mass range for weak-scale supersymmetry.

For the three cases samples of 70K, 25K, and 35K, respectively, of gluino and squark signal events was generated with a version of ISAJET containing all the MSSM decay modes.[3] The total production cross sections for all combinations of gluinos and squarks are

$$\begin{aligned} \text{Case I:} \quad & \sigma = 8.27\,\text{nb}\,, \\ \text{Case II:} \quad & \sigma = 7.60\,\text{nb}\,, \\ \text{Case III:} \quad & \sigma = 0.81\,\text{pb}\,. \end{aligned} \tag{3.2}$$

The Monte Carlo statistics are therfore small compared to those obtained in $10\,\text{fb}^{-1}$ for the first two cases but comparable in the third. This is reflected in the error bars on the plots shown below.

The signal events are characterized by multiple jets and large missing energy. For the lower masses in Cases I and II the dominant standard-model physics background comes from heavy flavors decaying into neutrinos, and the dominant detector-induced background comes from mismeasuring QCD jets. A total of 1.5M QCD jets of all types in twelve p_T ranges covering $50 < p_T < 3200\,\text{GeV}$ was generated with ISAJET to determine both kinds of backgrounds. For the high masses in Case III, the backgrounds from $W \to \ell\nu$ and

$Z \to \nu\bar{\nu}$ are also significant. A total of 40K $W \to \ell\nu$ and 80K $Z \to \nu\bar{\nu}$ events were generated covering the same p_T range.

The detector response to all events was simulated with **gemfast**,[7] a fast but realistic simulation of the GEM detector based on parameterizations of detailed GEANT simulations. For the barrel and endcap calorimeters the longitudinal and transverse shower profiles are generated using GFLASH,[8] modified to work outside the GEANT geometry environment. This describes not only the average shower profile but also profile fluctuations. The energy resolution is tuned to reproduce the results of full GEANT simulations for electromagnetic showers and for jets. The forward calorimeter, which covers $3 < |\eta| < 5.5$ with full measurement to $|\eta| \approx 5$, is crucial for the $\not{E}_T$ measurement but is not used for jets in this analysis. Hence, the simulation of individual cells is unnecessary. Instead, the energy and direction of each particle is smeared according to a parameterization derived from a mixture-level GEANT simulation[9] including:

- Energy resolution with a large constant term from $e/h > 1$, since no longitudinal weighting is used to reduce this;
- Angular resolution from shower spreading and from crossover to the opposite side of the beam pipe;
- Losses due to the beam hole, dead material, and calorimeter edges.

The resulting resolution is parameterized as a gaussian. Since the statistics of the detailed simulation were inadequate to study nongaussian tails, an additional 1% tail twice as wide as the main peak is added in accordance with DØ test beam data.[10] The effect of this nongaussian tail is small compared to the effects of angular resolution in the forward calorimeter and of the hole for the beam pipe, so its exact parameterization is not crucial. The missing energy vector is calculated using the cell energies in the barrel and endcap, the transverse energy measured in the forward calorimeter, and the momenta of detected muons.

In the inclusive $\not{E}_T$ cross section, the standard-model physics background is comparable to the signal, as can be seen in Fig. 1. Furthermore, the detector-induced background from mismeasured jets in the forward region is several times larger than the real background for small values of $\not{E}_T$.[11] Hence additional cuts are necessary. First consider the lower-mass Cases I and II. Since gluinos and squarks are centrally produced with $p_T \sim M$, they give multiple jets and "round" events in addition to $\not{E}_T$. Jets with $p_T > 75\,\text{GeV}$ were found using the **gemfast** fixed cone algorithm with $R = 0.7$. The minimum number of jets, N_{jet}, was varied. To identify round events, the sphericity in the transverse momentum plane, S_T, was calculated by summing all calorimeter cells with $E_T > 0.5\,\text{GeV}$ and $|\eta| < 3$. A cut on $S_T > 0.2$ provided good separation of signal and background, as can be seen from Fig. 2. After these cuts the signal to background ratio S/B for $\not{E}_T \sim 250\,\text{GeV}$ was about 3 for Case I and about 5 for Case II. The larger S/B for Case II reflects the harder $\not{E}_T$ spectrum from $\tilde{q}_R$ decays mentioned earlier.

Semileptonic decays of gluinos and squarks are important; see Section 4 below. However, a lepton veto improves by about a factor of two the S/B for the $\not{E}_T$ distribution by rejecting $t\bar{t}$ and other standard model backgrounds. Events were vetoed if they contained a muon or an isolated electron. An electron was identified as an isolated electromagnetic

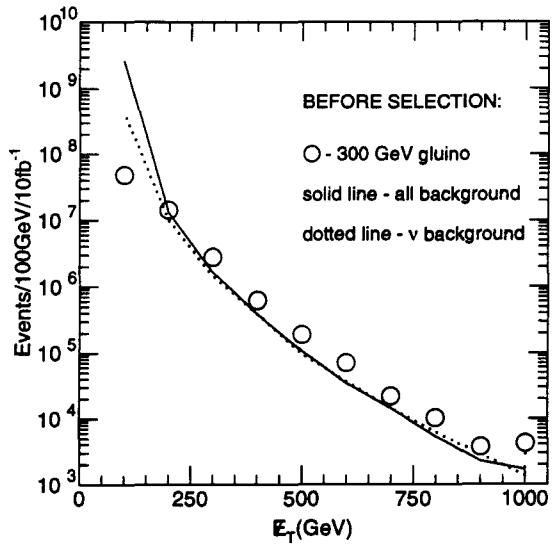

FIG. 1. Inclusive $\not{E}_T$ event numbers for Case I signal (circles), QCD background (dotted curve), and QCD background plus detector resolution (solid curve).

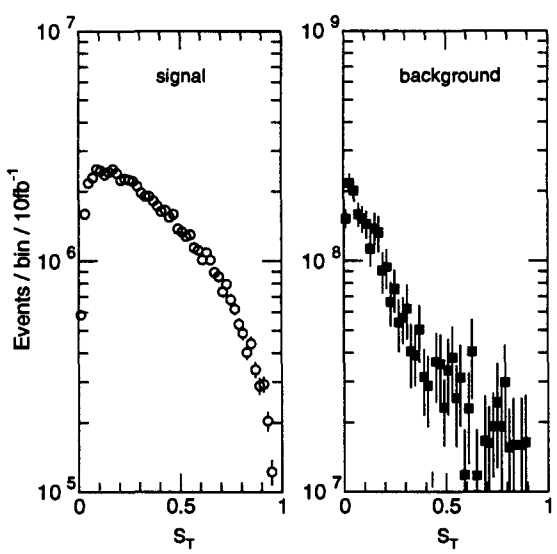

FIG. 2: Transverse sphericity distributions for Case I signal and for QCD background.

cluster in the calorimeter with $p_T > 20\,\mathrm{GeV}$ and $|\eta| < 2.5$, matched to a single track in the central tracker with loose matching constraint,

$$|E/p - 1| < \max(0.5, 3\sigma_p)\,. \tag{3.3}$$

Isolated muons with $p_T > 20\,\mathrm{GeV}$ and $\eta < 2.5$ were identified using the standard **gemfast** muon reconstruction. The efficiency of the lepton identification is not crucial for this

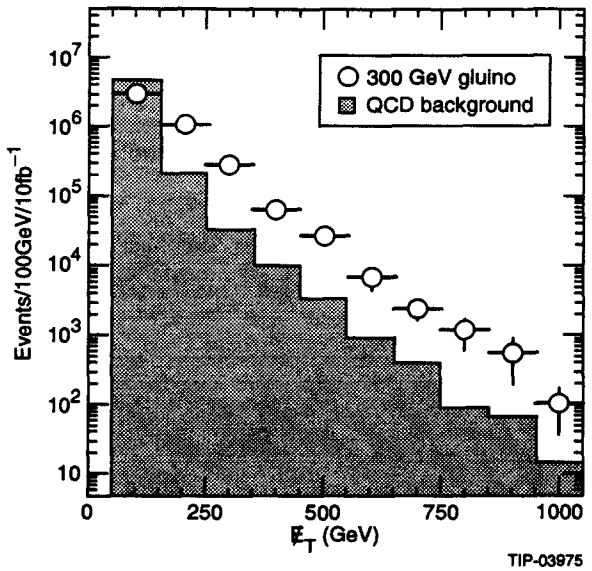

FIG. 3. $\not{E}_T$ signal for Case I MSSM parameters defined in Table 1 (open circles) and for QCD background (histogram) after requiring at least 5 jets with $p_T > 75$ GeV and the sphericity and lepton veto cuts described in the text.

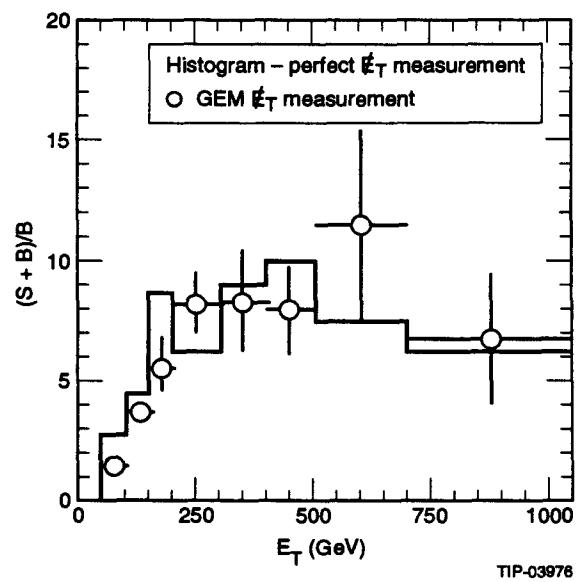

FIG. 4. Open circles: Ratio of signal and background curves from Fig. 3. Histogram: The same ratio for a perfect $\not{E}_T$ measurement.

analysis; even if it were perfect, there still would be background from τ-decays of b and t quarks.

The signal and background $\not{E}_T$ distributions for Case I with at least five jets and the sphericity and lepton veto cuts described above are shown in Fig. 3. The $(S+B)/B$ ratio, shown in Fig. 4, reaches about 8 for $\not{E}_T = 250$ GeV. Figure 4 also shows the $(S+B)/B$ ratio obtained using $\not{E}_T$ calculated from the the missing ν and $\tilde{\chi}_1^0$ momenta, with the rest of the analysis unchanged. While the GEM calorimeter performance increases the background

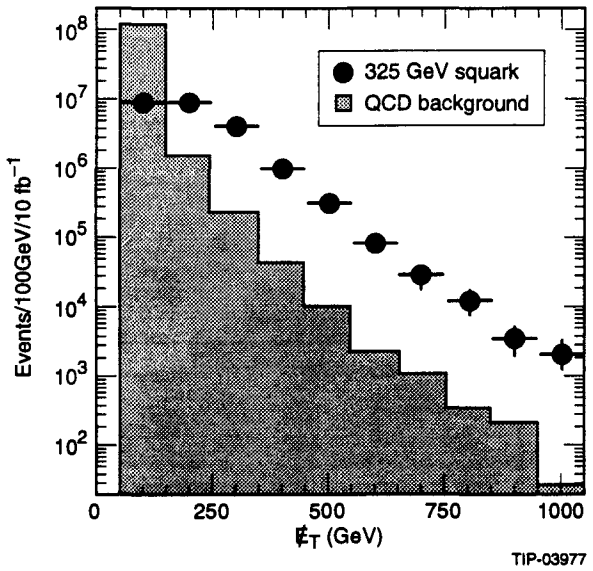

FIG. 5. $\not{E}_T$ signal for Case II MSSM parameters defined in Table 1 (solid circles) and for QCD background (histogram) after requiring at least 2 jets with $p_T > 75$ GeV and making the sphericity and lepton veto cuts described in the text.

at low $\not{E}_T$, it provides reasonable agreement with the perfect detector result in the region for which the ratio is large. The $(S+B)/B$ ratio is larger than that found previously[6] after similar cuts, partly because both gluinos and squarks are now included, and partly because the description of the decays has been improved and the other MSSM parameters are slightly different. For the same physics assumptions used before, the new simulation gives $(S+B)/B \approx 4$. This is somewhat smaller than found previously, reflecting the larger beam pipe and the more realistic description of the central and endcap calorimeters.

Figure 5 shows the signal and background for Case II, requiring at least two jets with $p_T > 75$ GeV and the same sphericity and lepton veto cuts. For this case the direct decay $\tilde{q}_R \to \tilde{\chi}_1^0 q$ dominates and leads to a significantly harder $\not{E}_T$ spectrum and to lower jet multiplicity. The $(S+B)/B$ ratio is even larger in this case.

Figure 6 plots the signals for Cases I and II and the standard model the background for $\not{E}_T > 250$ GeV and $S_T > 0.2$ vs. the minimum number, $N_{\rm jet}$, of jets with $p_T > 75$ GeV. Both signals and backgrounds are constant for $N_{\rm jet} \leq 2$. It is impossible to have a large sphericity with only one jet. The signal falls off faster with increasing $N_{\rm jet}$ for Case II than for Case I because $\tilde{q}_R \to \tilde{\chi}_1^0 q$ is dominant and gives a large rate for two jets plus $\not{E}_T$. Thus, the $N_{\rm jet}$ dependence provides a handle to distinguish among models. Figure 7 shows the dependence of $(S+B)/B$ on $N_{\rm jet}$ and shows that the choices $N_{\rm jet} = 5$ and 2 given above for Cases I and II respectively give favorable signal to background ratios.

Given the large number of signal events, the statistical significance of the signals is not an issue. The t, W and Z backgrounds can be checked using isolated lepton samples; the b and c backgrounds can be checked using muons in jets. The $\not{E}_T$ resolution of the detector can be studied using inclusive data on QCD jets and on γ + jets events. While the detector effect is larger than in the less realistic Baseline I design, it is still not the dominant problem. Given all these constraints, the background should be reliably known,

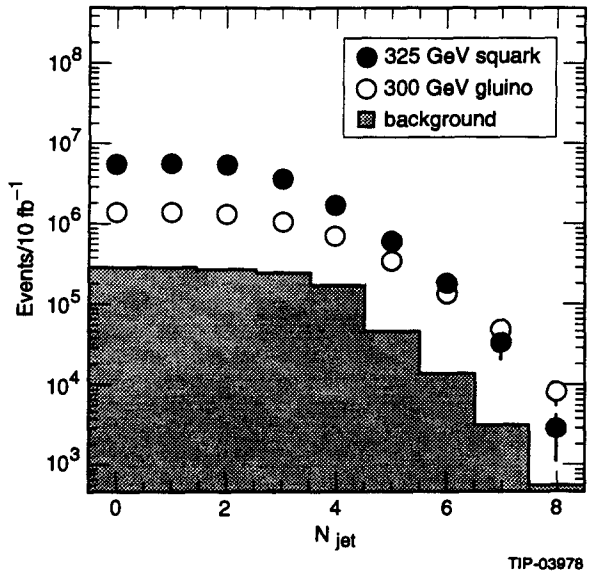

FIG. 6. Event numbers with $\not{E}_T > 250\,\mathrm{GeV}$ and the sphericity and lepton veto cuts described in the text vs. the minimum number N_{jet} of jets with $p_T > 75\,\mathrm{GeV}$. Open circles: Case I signal. Solid circles: Case II signal. Histogram: QCD background. Case II has more events with low jet multiplicity because $\tilde{q}_R \to \tilde{\chi}_1^0 q$ dominates.

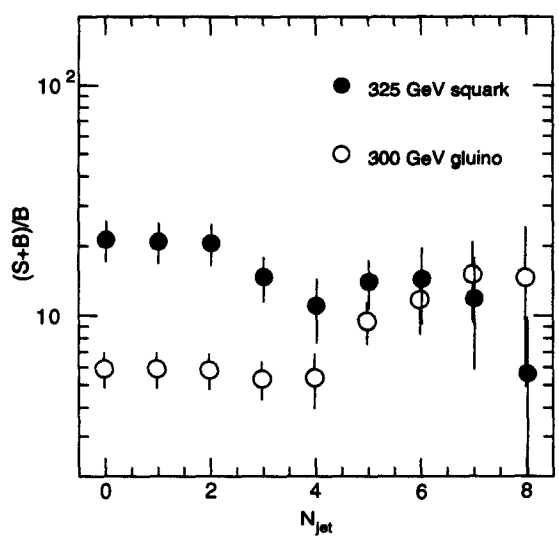

FIG. 7. Ratio $(S+B)/B$ for Case I (open circles) and Case II (solid circles) vs. the minimum number of jets N_{jet} in the event. The values $N_{\mathrm{jet}} = 5$ and 2 are optimal for the two cases.

so observation of a signal 5–10 times that expected from the standard model should be very convincing. The difficult problem of extracting the masses and other model parameters is briefly discussed in Section 5.

For heavy gluino and squark masses such as those in Case III, $\not{E}_T$ is so large that the $\not{E}_T$ resolution is not important. Figure 8 shows the signal and background $\not{E}_T$ distributions

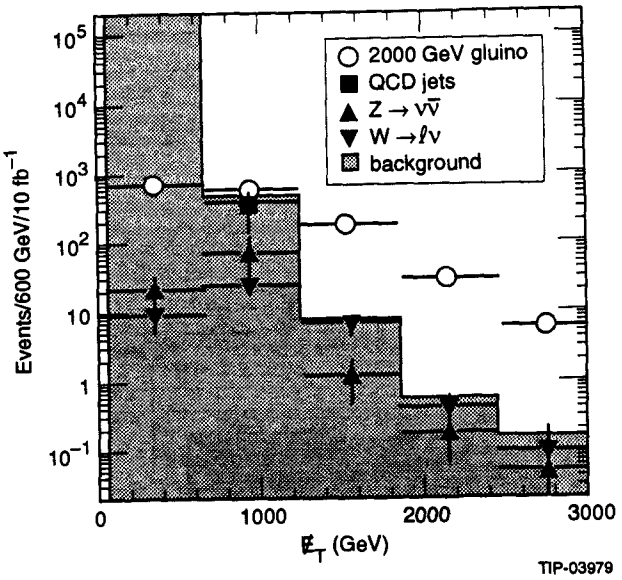

FIG. 8. $\not{E}_T$ signal for Case III MSSM parameters defined in Table 1 after requiring at least 4 jets with $p_T > 300\,\mathrm{GeV}$ and making the sphericity and lepton veto cuts described in the text. Open circles: Signal. Solid squares: QCD background. Triangles: $W \to \ell\nu$ and $Z \to \nu\bar{\nu}$ backgrounds. Histogram: Sum of all backgrounds.

for Case III with at least four jets having $p_T > 300\,\mathrm{GeV}$ and with the sphericity and lepton veto cuts identical to those for lighter masses. Heavy flavor backgrounds, detector-induced backgrounds from mismeasured QCD jets, and W and Z backgrounds are included. The QCD background dominates for low $\not{E}_T$ but falls more rapidly than the W and Z backgrounds, and both must be considered. Since several hundred signal events survive these cuts with large S/B, it is evident that GEM could discover SUSY in this channel up to masses of order 2 TeV, about the upper limit if SUSY is related to electroweak symmetry breaking. For such heavy masses the ability to run at high luminosity may be important.

4. Leptonic Signatures

In addition to the $\not{E}_T$ plus multi-jet signatures described above, there are many other signatures for supersymmetry, including a number involving two or more leptons.[12] In particular, since the gluino is a self-conjugate Majorana fermion, $\widetilde{g}\widetilde{g}$ and $\widetilde{g}\widetilde{q}$ pairs can give isolated $\ell^\pm\ell^\pm$ pairs. Observing such likesign pairs is essential for establishing the Majorana nature of any gluino signal. It also helps in separating gluinos and squarks. The dominant standard model $\ell^\pm\ell^\pm$ background is expected to be from $t\bar{t}$ events in which either a $b \to \ell X$ lepton appears isolated or an isolated lepton sign is wrongly determined. These backgrounds, calculated previously in Ref. 12, are found to be negligible. For light gluinos, such as those in Cases I and II, the cross sections are so large that one can rely only on the $\mu^\pm\mu^\pm$ channel, for which the lepton signs are very well determined in GEM. Therefore, only the issue of measuring the signs of electrons from Case III is addressed here.

The same sample of Case III signal events described in the previous section was used for this analysis. While it is possible to enhance the leptonic sample by forcing a particular decay chain, e.g. $\widetilde{g} \to \widetilde{\chi}_1^\pm q\bar{q}'$, $\widetilde{\chi}_1^\pm \to \widetilde{\chi}_1^0\ell^\pm\nu$, there are many such chains possible, no one

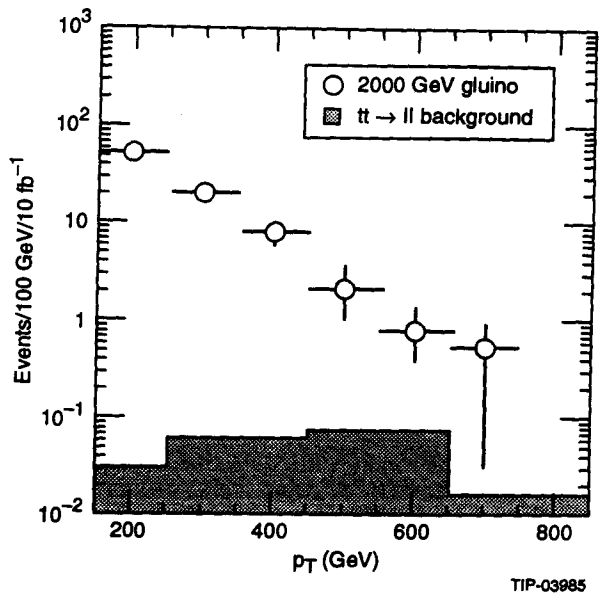

FIG. 9. p_T distributions for the highest-p_T isolated lepton in dilepton events containing two isolated like-sign leptons. Open circles: Signal events generated with Case III MSSM parameters. Histogram: $t\bar{t}$ background from mismeasured electrons in the GEM central tracker.

of which obviously dominates. It was therefore decided to use the inclusive sample. For the background, only $t\bar{t}$ events, which are expected to dominate, were considered. A total sample of 30K $t\bar{t}$ events in ten bins with $50 < p_T < 3200\,\mathrm{GeV}$ were generated, forcing the decays $t \to e^+\nu_e b$ and $\bar{t} \to \mu^-\bar{\nu}_\mu X$. This sample was used to determine the principal detector-induced background, that from misidentification of $e^\pm$ signs in the central tracker. From this, the total $\ell^\pm\ell^\pm$ background was determined.

Electrons and muons with $p_T > 50\,\mathrm{GeV}$ and $|\eta| < 2.5$ were identified using the relatively loose cuts described in the previous section. These cuts, optimized for background rejection rather than for signal detection, appear to be adequate to identify this signal. At least two such leptons were required satisfying the isolation criterion

$$\sum_{R=0.2}{}' E_T < 0.1 p_{T\ell} + 5\,\mathrm{GeV}\,. \tag{4.1}$$

Here, the prime on the sum indicates that the lepton itself is not included. This cut effectively rejects[12] the background from $t \to \ell^+\nu b$ and $\bar{t} \to \bar{b}X$, $\bar{b} \to \ell^+X$. In addition a missing energy $\not{E}_T > 500\,\mathrm{GeV}$ and a transverse sphericity $S_T > 0.2$ were required. After these cuts, the total dilepton rates for the signal and for the $t\bar{t}$ background were comparable, so a very large rejection of unlike-sign pairs is not needed.

Figure 9 shows the transverse momentum distribution of the highest p_T lepton in likesign dilepton events satisfying the above cuts. The lepton spectrum is soft relative to the gluino mass because the leptons arise from cascade decays. Figure 9 also shows the $t\bar{t} \to \ell^+\nu b\ell^-\bar{\nu}\bar{b}$ background in which an electron sign is mismeasured by the GEM central tracker. The probability of mismeasurement was determined using the **gemfast** parameterization of the central tracker electron resolution, including the tail from bremsstrahlung.[7] Muon signs are assumed perfectly determined, an excellent approximation at these momenta.

Since the cuts not dependent on the electron sign reduce the background to the order of the signal, and since most of the signal leptons have $p_T < 600\,\mathrm{GeV}$, for which the central tracker determines signs with 95% reliability, it is not surprising that the background is small compared to the signal. The signal comprises several tens of events per $10\,\mathrm{fb}^{-1}$ when both electrons and muons are combined. It would be uncomfortably small if one had to rely on only the $\mu^\pm\mu^\pm$ signal, which is a factor of four smaller. Thus, the ability to identify electron signs improves the performance of GEM for this physics.

5. SUSY Parameter Determination

In the MSSM there are at least eight mass parameters ($M_{\tilde{g}}$, $M_{\tilde{q}}$, $M_{\tilde{t}_L}$, $M_{\tilde{t}_R}$, $M_{\tilde{\ell}_L}$, $M_{\tilde{\ell}_R}$, $M_{\tilde{\nu}_L}$, and M_A), two additional parameters related to the Higgs sector (μ and $\tan\beta$), and still more parameters related to $\tilde{t}$ decay. Non-minimal SUSY models have even more parameters. Of course it is possible to relate many of these parameters by making more theoretical assumptions.[4,5] Since all supersymmetric particles in the MSSM ultimately decay into the $\tilde{\chi}_1^0$, which is invisible, it is not possible to reconstruct any masses directly.

The approximate mass scale can be inferred from the $\not{E}_T$ scale at which the signal deviates from the standard model background, as can be seen by comparing Figs. 3, 5, and 8. The mean $\not{E}_T$ for the distribution of the excess of events can be calculated very accurately for low masses because of the high statistics. However, the relationship of this mean to the masses is model dependent. For example, the missing energy is lower and the jet multiplicity is higher if $M_{\tilde{q}} > M_{\tilde{g}}$ than if $M_{\tilde{g}} > M_{\tilde{q}}$.

There are a large number of possible signatures to use to determine the parameters. These include the $\not{E}_T$ cross section with multiple leptons,[12] multilepton cross sections arising from production of $\tilde{\chi}_1^\pm\tilde{\chi}_2^0 \to 3\ell$ and similar channels, and the observed cross sections or limits for $h, H \to \gamma\gamma$; $h, H \to 4\ell$; and $t \to H^+ b$. The tools to simulate these signatures have recently been developed,[3] and the methods to determine all of the MSSM parameters from these signatures are being studied. However, it is clear from the previous two sections that GEM is capable of observing clean samples of events in the relevant channels.

We would like to thank Tomasz Skwarnicki, Mike Shupe, and all our other GEM colleagues whose work on simulations made this study possible.

References

1. GEM Collaboration (B. Barish et al.), *Technical Design Report*, GEM-TN-93-262 (1993).
2. For reviews, see H. E. Haber and G. L. Kane, Phys. Rept. **117**, 75 (1985); S. Dawson, E. Eichten and C. Quigg, Phys. Rev. **D31**, 1581 (1985).
3. H. Baer, F.E. Paige, S.D. Protopopescu and X. Tata, FSU-HEP-930329 (1993).
4. R. Arnowitt and P. Nath, Phys. Rev. Lett. **69**, 725 (1992).
5. R. Ross and R. Roberts, Nucl. Phys. **B377**, 571, 1992.
6. GEM Collaboration (B. Barish et al.), *GEM Responses to the December 1991 PAC Report*, GEM TN-92-131, (July 8, 1992).

7. T. Skwarnicki, GEM Technical Note, in preparation. See also Ref. 1, Section 2.2.
8. G. Grindhammer, et al., Proc. of the Workshop on Calorimetry for the Supercollider, Tuscaloosa, AL, 1989, p.151, SLAC-PUB-5072, 1989 and Nucl. Inst. and Meth. **A290**, 469 (1990).
9. Ref. 1, Section 5.2.
10. J. Womersley, private communication.
11. F. E. Paige and A. Vanyashin, GEM TN-92-70 (1992).
12. H. Baer, X. Tata and J. Woodside, Phys. Rev. **D45**, 142 (1992).